OPEN ACCESS Science International

ISSN 2305-1884
DOI: 10.17311/sciintl.2016.39.50

Research Article
A Study of Concentration and Temperature Dependent Effect on Speed of Sound and Acoustical Parameters in Zinc Oxide Nanofluid

Vijayta Gupta, Upasna Magotra, Sandarve, Amit Kumar Sharma and Meena Sharma

Department of Chemistry, University of Jammu, Jammu and Kashmir-180006, India

Abstract
Ultrasonic propagation through nanofluids has now become a subject of great interest. It is a typical technique to examine the structure formation in nanofluid. Speed of sound can be considered to evaluate acoustical parameters and hence, to investigate physico-chemical properties of nanofluid. Investigation of these physico-chemical properties enables to understand the nature and strength of particle-particle and particle-fluid interactions. Zinc oxide nanoparticles are synthesized by co-precipitation method, while ZnO-ethylene glycol nanofluids are prepared with the aid of sonication. Characterization of synthesized nanoparticles are carried out by XRD, FTIR, UV-visible, TEM, SEM and EDX spectroscopic techniques. Speed of sound, density and viscosity values are measured for different concentrations of ZnO nanofluids at 298.15, 303.15 and 308.15 K. Different acoustical parameters, such as adiabatic compressibility (β_{ad}), intermolecular free length (L_f), relaxation time (τ), absorption coefficient (α/f^2), acoustic impedance (Z), Gibb's free energy (ΔG) and free volume (V_f) are evaluated from the experimental data. Variation in these acoustical parameters helps to know the mechanism of cluster formation and or interaction between particles in the ZnO nanofluids. It is found that particle-fluid interaction increases up to a critical concentration of 0.6 wt% beyond, which there is predominance of particle-particle interaction.

Key words: Ultrasonic, nanofluids, acoustical parameters, interactions, characterization

Received: March 03, 2016 **Accepted:** March 10, 2016 **Published:** March 15, 2016

Citation: Vijayta Gupta, Upasna Magotra, Sandarve, Amit Kumar Sharma and Meena Sharma, 2016. A study of concentration and temperature dependent effect on speed of sound and acoustical parameters in zinc oxide nanofluid. Sci. Int., 4: 39-50.

Corresponding Author: Vijayta Gupta, Department of Chemistry, University of Jammu, Jammu and Kashmir-180006, India

Competing Interest: The authors have declared that no competing interest exists.

Data Availability: All relevant data are within the paper and its supporting information files.

INTRODUCTION

Nanofluids represent the technology of heat transfer fluids, where the heat transfer properties of conventional base fluids are improved by the addition of nanoparticles to form stable dispersions. Nanofluids are colloids engineered by dispersing solid nanoparticles in base liquids such as water, glycols, lubricants and light oils[1]. These represent two-phase systems, in which one phase i.e., solid phase is present in another phase i.e., liquid phase. In 1995, Choi, a scientist of Argonne Laboratory (USA) proposed the concept of nanofluid[2]. Nanofluids can be synthesized by simultaneously synthesizing the nanoparticles and dispersing the particles directly into the base fluid, which is single step technique. This method leads to the preparation of stable nanofluid as the method does not involve processes, such as drying, storage, transportation and dispersion of nanoparticles. This results in minimization of agglomeration of nanoparticles and enhancement of stability of fluids[3]. Single step methods involve methods like direct evaporation technique, submerged arc nanosynthesis, the polyol method and the microwave method[4-6]. However, only low vapor pressure fluids can be used in single step method. Moreover, the process is costlier and has disadvantages of small scale production and residual reactant in the base fluid. On the other hand, two-step technique is used method for preparing nanofluids. Nanoparticles are initially synthesized as a dry powder by chemical or physical techniques and are then dispersed into the base fluid. However, agglomeration of nanoparticles makes the nanofluid unstable. So, maintaining stability of nanofluids is a big challenge. In general, stability of suspension can be obtained by using surface activators and/or dispersants, changing the pH value of suspension and using ultrasonic vibration[7]. In order to prepare stable nano-suspension, ultrasonication is an accepted technique used to disperse aggregated nanoparticles[8].

Nanofluids are found to have high conduction of heat than base fluid[4,9-11]. Since heat transfer takes place on the surface of the base fluid, more surface area of nanoparticles compared to their volume, Brownian motion and interparticle forces causes enhancement in thermal conductivity of nanofluids[12-18]. Study of nanofluids are fundamental for different types of heat transfer management systems. Therefore, it is important to examine the movement of nanoparticles in nanofluids. Ultrasonic propagation in a nanofluid is a typical way to investigate the structure formation without any prior modifications of the sample. Speed of sound can be measured to determine acoustical parameters and hence, to study physico-chemical properties of nanofluid. Study of these physico-chemical properties helps in understanding the nature and strength of molecular interactions. These intra and inter molecular interactions in a liquid system is very important to have an idea about the interacting properties of the molecules. Several studies have been performed to investigate the properties of ultrasonic propagation in nanofluid prepared in polar or non-polar base fluids[19-30].

In the present study, variation in speed of sound as a function of concentration of nanoparticles for different temperature of ZnO nanofluids prepared in ethylene glycol are reported. Using the results of speed of sound, density and viscosity measurement and various acoustical parameters were derived to understand the effect of concentration and temperature. This helps to realize the mechanism of cluster formation and or interaction between particles in the ZnO nanofluids. The ZnO nanofluids are prepared using two-step method with ethylene glycol as base fluid. Ethylene glycol is used as solvents, carriers, lubricants, binders, bases and coupling agents and also for extraction, separation and purification of materials in industrial fields[31]. The ZnO nanoparticles have received much interest due to their promising properties that makes it applicable in many devices, such as solar cells, electroluminescent devices, electrochromic windows and chemical sensors[32]. Moreover, ZnO nanoparticles display a high extent of cancer cell selectivity[33]. The ZnO nanoparticles also have antimicrobial, UV blocking, high catalytic and photochemical activities[34]. Hence, ultrasonic wave technique is used to study the effect of particle concentration and temperature on the speed of sound in ZnO nano-suspensions in Ethylene Glycol (EG). The acoustical parameters calculated are used to analyze the interactions present in the nanofluid system and the results are discussed.

MATERIALS AND METHODS

Synthesis: The precursors used in the synthesis of ZnO nanoparticles are zinc acetate [$Zn(CH_3COO)_2.2H_2O$] and sodium hydroxide. A 0.5 M aqueous solution of zinc acetate was kept under constant stirring using magnetic stirrer at 80°C to completely dissolve for 1 h. After complete dissolution of zinc acetate, 2.5 M NaOH aqueous solution was added under high speed constant stirring drop by drop (slowly for 45 min) touching the walls of the vessel till the pH reaches to 12. The reaction between zinc acetate and sodium hydroxide solution is as follows:

$$Zn(CH_3COO)_2 + 2\,NaOH \text{ ----------> } Zn(OH)_2 + 2\,NaNO_3$$

$$Zn(OH)_2 \text{ ----------> } ZnO + H_2O$$

The reaction was allowed to proceed for 2 h after complete addition of sodium hydroxide. After the completion of reaction, the solution was allowed to settle for overnight and further, the supernatant solution was separated carefully. The remaining solution was centrifuged for 10 min and the precipitate was removed. Thus, precipitated ZnO NPs were washed three times with triply distilled water and ethanol to remove the byproducts, which were bound with the precipitate and then dried in oven at about 60°C. The white powder obtained is subjected to calcinations at 600°C for 3 h.

Zinc oxide nanofluids of different concentrations (0.2, 0.4, 0.6, 0.8 and 1% by weight) were prepared by dispersing a specified amount of zinc oxide nanoparticles in ethylene glycol followed by sonication. A special thermostatic water bath instrument was used for speed of sound, density and viscosity measurements. Multi frequency ultrasonic interferometer (Model F81, Mittal Enterprises, New Delhi) was used to measure speed of sound of ultrasonic waves through the nanofluid samples with an accuracy of ±0.05% at frequency of 6 MHz. Density of the fluid was determined using specific gravity bottle (5 cc) with accuracy of ±2 parts in 10^4. Viscosity of the fluid was measured by Ostwald viscometer. The accuracy of viscosity in this method is ±0.001 N sec m^{-2}. All these measurements were performed for fluids of all concentrations at three different temperatures of 298.15, 303.15 and 308.15 K. The speed of sound, density and viscosity measurements were repeated several times for accuracy and the average of the continuous consistent values are reported in this study.

Characterization: The crystalline structure, phase composition and crystallite size of ZnO were identified from XRD patterns obtained using Cu Kα radiation (λ = 1.541 Å) for 2θ value ranging from 10-100° in x-ray diffractometer (Bruker AXS D8 Advance). Fourier transform infrared spectra of zinc oxide nanoparticles were recorded using Model RZX (PerkinElmer) spectro photometer with KBr pellet technique from 4000-400 cm^{-1}. The UV-visible absorption spectrum was recorded using Lambda 750 PerkinElmer UV-VIS-NIR spectrophotometer for optical characterization. The size and morphology of nanoparticle is found using transmission electron microscope (Hitachi (H-7500) microscope) operating at 80 kV. Powder sample for TEM measurements is suspended in ethanol and ultrasonically dispersed. Drops of the suspensions are placed on a copper grid coated with carbon. The morphology of the particles are observed by a scanning electron microscope (SEM-EDS) using SEM make JEOL Model JSM-6390LV and EDS make JEOL Model JED-2300 with an accelerating voltage of 20 kV.

RESULTS AND DISCUSSION

Structural studies: Figure 1 shows the XRD pattern of prepared ZnO NPs that clearly exhibits the crystalline nature of this material. The peaks at scattering angles 2θ = 31.9, 34.7 36.5, 47.8, 56.8, 63.1, 66.6, 68.1 and 69.3° corresponds to (100), (002), (101), (102), (110), (103), (200), (112) and (201) crystal plane, respectively. The peaks of the obtained product are corresponding to the hexagonal phase (wurtzite structure) of zinc oxide reported in standard JCPDS card No. 36-1451[35] with lattice constants a = b = 3.22 Å, c = 5.24 Å. The crystallite size has been estimated from the XRD pattern using the Scherrer's Eq. 1[36]:

$$D = \frac{K\lambda}{\beta Cos\theta} \quad (1)$$

where, K is a constant (0.9), λ is the x-ray wavelength used in XRD (0.154 nm), θ is the bragg angle and β is the FWHM (Full width at half maximum intensity), that is broadening due to the crystallite dimensions. The average crystallite size of ZnO NPs was found to be around 32.68 nm. Figure 2 shows the FTIR spectra of ZnO nanoparticles. A broad absorption band was observed between 550 and 465 cm^{-1} with shoulder shape. This broad band is characteristic of hexagonal ZnO phase[37]. There were several small absorption bands at ~3438, ~2342 and ~1624 cm^{-1}. These absorption bands were likely related to H_2O (O-H) and CO_2 (C-O) absorbed from the atmosphere (air) and can therefore be neglected.

Figure 3a shows the absorption spectrum of ZnO sample calcined at a temperature of 600°C. A typical exciton absorption at ~380 nm is observed in the absorption spectrum, which can be assigned to the intrinsic band-gap absorption of ZnO due to the electron transitions from the valence band to the conduction band ($O_{2p} \rightarrow Zn_{3d}$)[38-40]. The absorption peak for 5-6 nm ZnO nanoparticles has been found to be between 360 and 365 nm[32,41]. The variation in absorption peak is due to variation in particle size. In order to calculate the optical band gap of sample by using Tauc's relation in the following Eq. 2[42]:

$$(Ah\nu)^n = B\,(h\nu - E_g) \quad (2)$$

where, hν is photon energy, A is absorption coefficient, B is a material constant and n is either 2 for a direct band gap material or ½ for an indirect band gap materials. Figure 3b shows the variation of $(Ah\nu)^2$ versus photon energy, hν for ZnO nanoparticles. Extrapolating the linear portion of the curve to absorption equal to zero gives the value of the

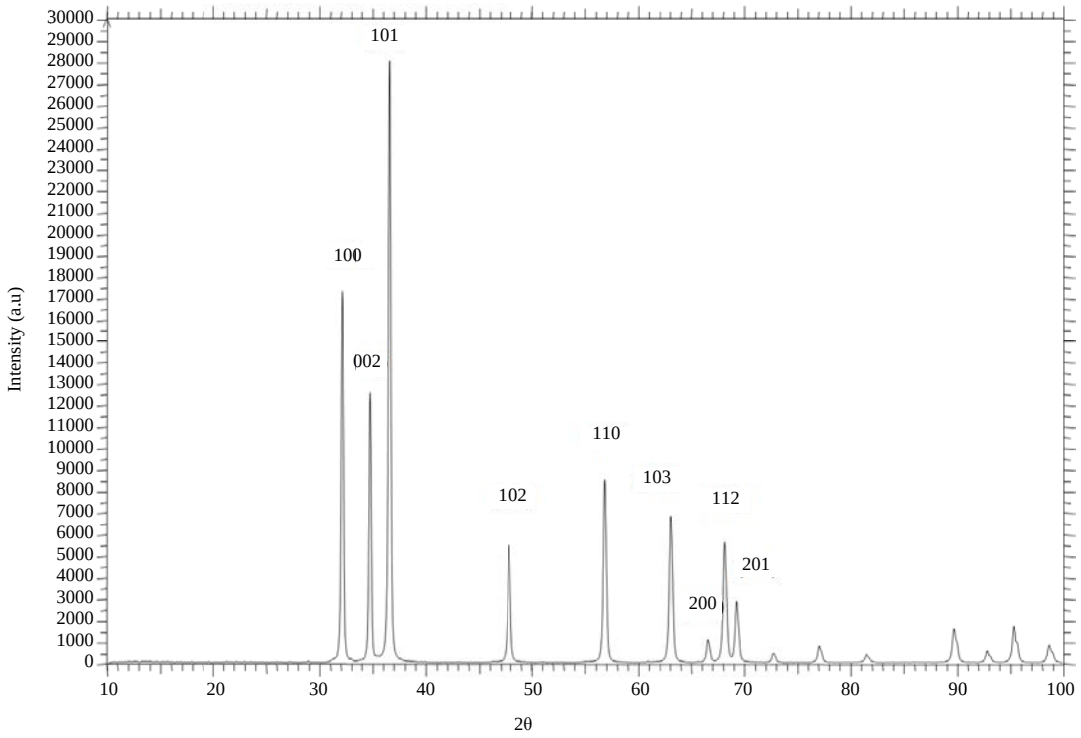

Fig. 1: XRD patterns showing peaks corresponding to hexagonal phase (wurtzite structure) of ZnO nanoparticles, XRD: X-ray powder diffraction

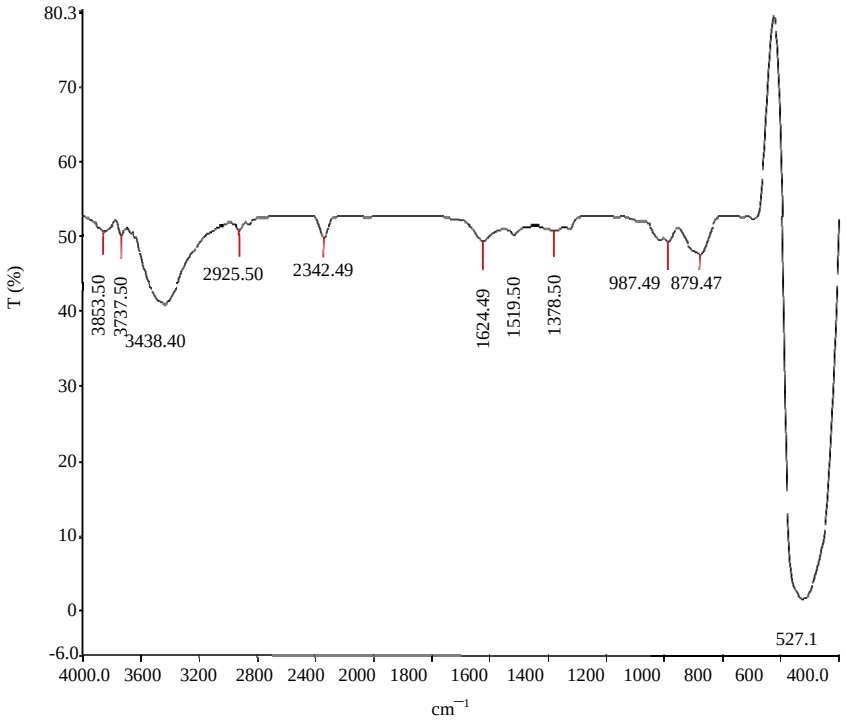

Fig. 2: A broad absorption band between 550 and 465 cm^{-1} in FTIR spectra corresponds to stretching vibration of ZnO bond, FTIR: Fourier transform infrared spectroscopy

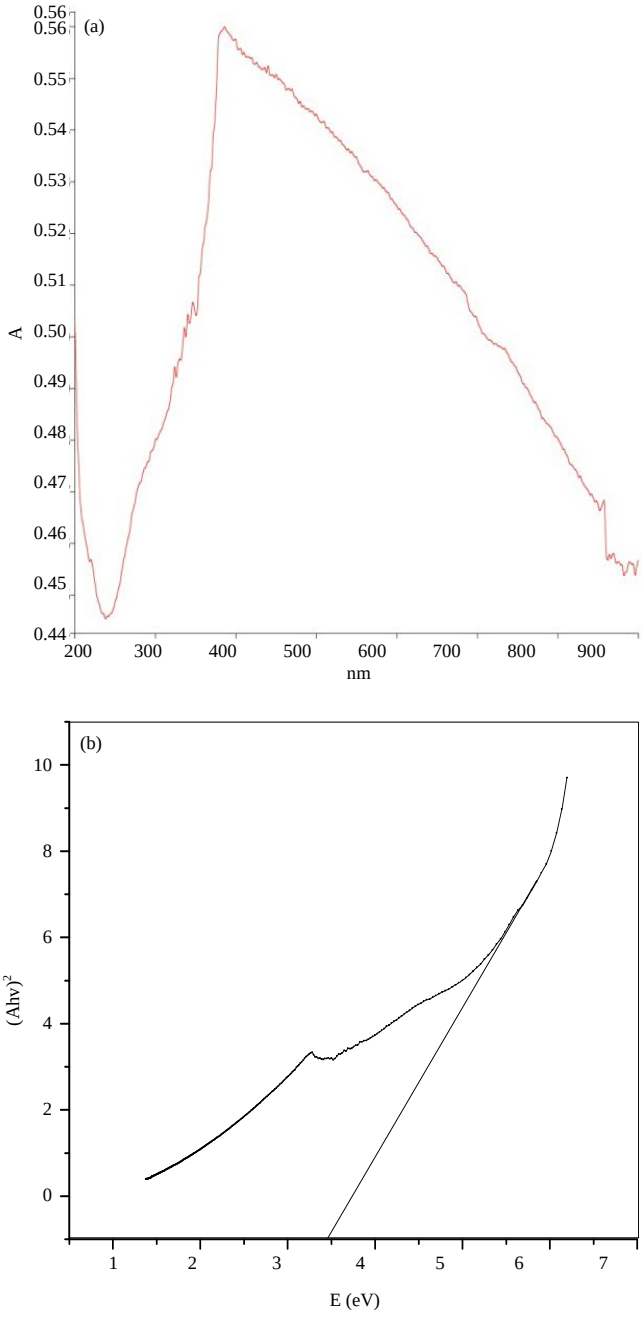

Fig. 3(a-b): Plots of (a) Absorption band at ~380 nm in UV-VIS spectra of nano ZnO can be attributed to the electron transitions from the valence band of oxygen to the conduction band of Zn and (b) $(Ahv)^2$ versus hv for nano ZnO synthesized by calcining at 600°C. Extrapolation of the plot shows band gap equal to 3.47 eV, which is greater than band gap of bulk ZnO[43]

direct band gap to be 3.47 eV. This value is higher than that of 3.3 eV reported in the literature[43]. Band gap energy increases with decreasing particle size due to quantum size effects[44].

Figure 4 reveals the TEM image of ZnO nanoparticles. This image reveals that the product consist of approximate spherical particles with the average size of 28-43 nm, which is in close agreement with that estimated by Scherrer equation based on the XRD pattern. It can be observed that ZnO nanoparticles mainly present granules with approximate spherical shape and are well crystallized[40]. Figure 5 shows the

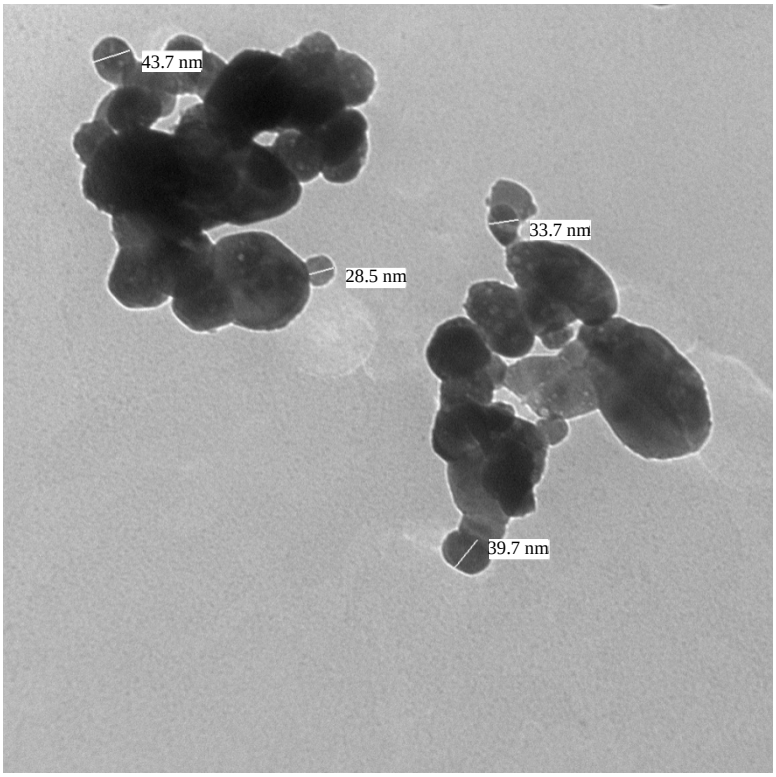

Fig. 4: TEM micrograph of nano ZnO showing approximate spherical shape of ZnO nanoparticles with average size lying between 28 and 43 nm, TEM: Transmission electron microscopy

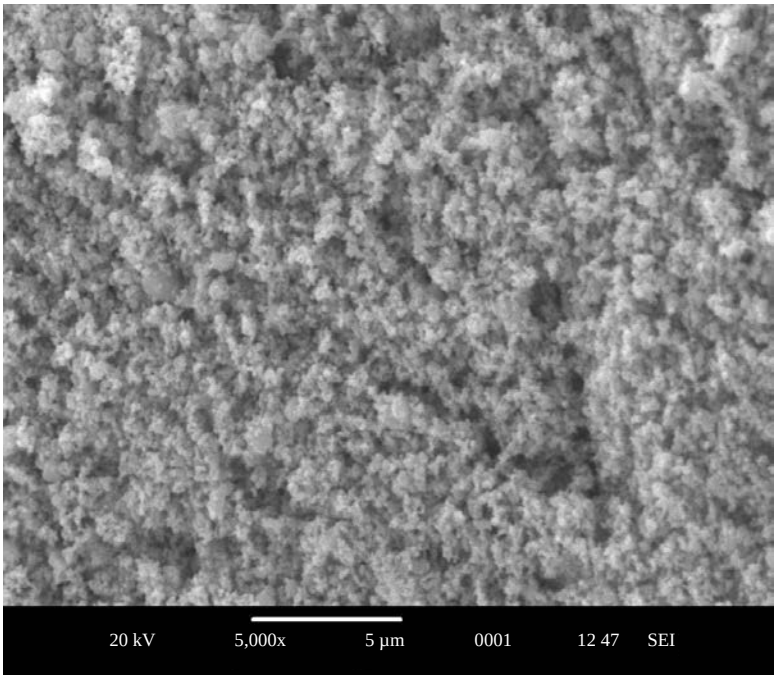

Fig. 5: Aggregations of spherically shaped ZnO nanoparticles seen in SEM micrograph analysis, SEM: Scanning electron microscopy

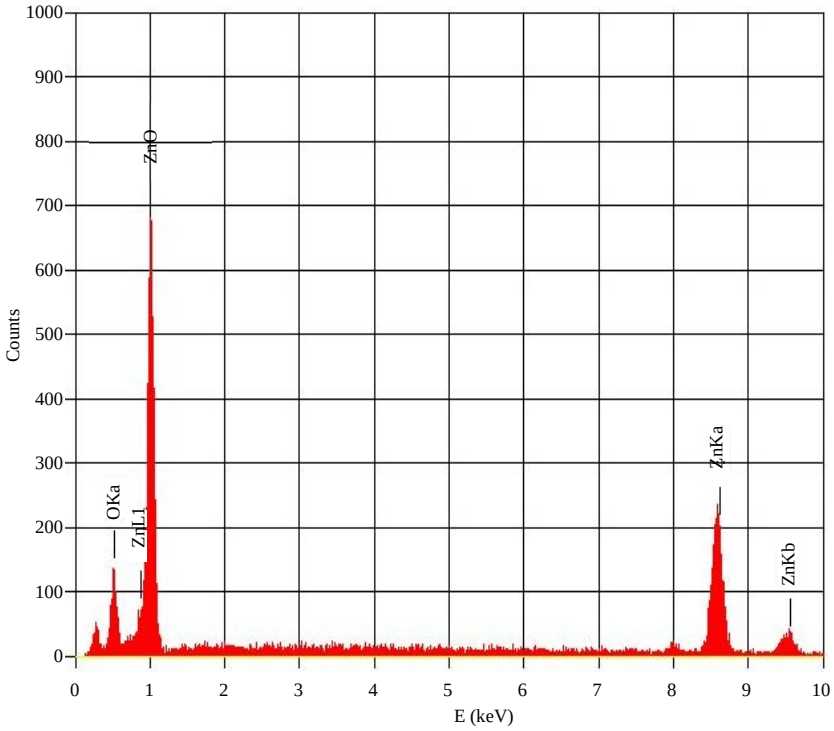

Fig. 6: EDX spectra shows the peaks corresponding to the presence of Zn and O elements in the prepared sample of ZnO, EDX: Energy-dispersive x-ray spectroscopy

Table 1: Speed of sound and density of ZnO nanofluids at 298.15, 303.15 and 308.15 K

	$U\times10^{-3}$ (m sec^{-1})			$\rho\times10^{-3}$ (kg m^{-3})		
Concentration (wt%)	298.15 K	303.15 K	308.15 K	298.15 K	303.15 K	308.15 K
0	1.6548	1.6416	1.6236	1.1098	1.1063	1.1028
0.2	1.6644	1.6500	1.6320	1.1080	1.1049	1.1005
0.4	1.6752	1.6596	1.6404	1.1095	1.1071	1.1029
0.6	1.6920	1.6740	1.6512	1.1124	1.1097	1.1058
0.8	1.6776	1.6656	1.6416	1.1147	1.1123	1.1087
1	1.6716	1.6572	1.6308	1.1180	1.1151	1.1108

SEM micrograph of the ZnO nanoparticles at 5,000x magnification. The SEM micrograph indicates a homogeneous shape and size for ZnO nanoparticles and aggregations of chemically synthesized nanoparticles. The EDX spectrum of ZnO NPs is given in Fig. 6. The EDX spectra result shows that there are no other elemental impurities present in the prepared ZnO NPs.

Ultrasonic studies: Various acoustical parameters[45] like adiabatic compressibility (β_{ad}), intermolecular free length (L_f), relaxation time (τ), absorption coefficient (α/f^2), acoustic impedance (Z), Gibb's free energy (ΔG) and free volume (V_f) have been evaluated using speed of sound (U), density (ρ) and viscosity (η) data for ZnO nanofluids.

The speed of sound of ultrasonic waves in the liquid can be calculated by the Eq. 3:

$$U = \lambda x f \ \text{m sec}^{-1} \quad (3)$$

where, f is the frequency of the generator and λ is the wavelength of ultrasonic waves in the liquid.

Speed of sound measured for pure ethylene glycol and prepared ZnO nanofluids at three different temperatures and different concentration is presented in Table 1. It is evident that the speed of sound in ZnO nanofluid increases to a maximum value upto 0.6 wt% beyond, which it starts decreasing at all the temperatures, the value being higher at 298.15 K and lower at 308.15 K. This increase in speed of sound upto 0.6 wt% may be due to small size and more surface area of nanoparticles resulting in increased adsorption of nanoparticles on the surface of ethylene glycol molecules. This increased adsorption may cause strong interaction between particles and fluid molecules[46] in naofluid matrix and

Table 2: Viscosity and adiabatic compressibility of ZnO nanofluids at 298.15, 303.15 and 308.15 K

	$\eta \times 10^3$ (N sec m^{-2})			$\beta_{ad} \times 10^{10}$ (N^{-1} m^2)		
Concentration (wt%)	298.15 K	303.15 K	308.15 K	298.15 K	303.15 K	308.15 K
0	17.2500*	13.8600*	11.6400*	3.2905	3.3542	3.4399
0.2	16.1369	12.9812	10.9764	3.2580	3.3244	3.4117
0.4	15.8206	12.7610	10.8370	3.2117	3.2795	3.3695
0.6	15.3903	12.5117	10.6188	3.1401	3.2158	3.3168
0.8	15.7805	12.9024	10.8919	3.1876	3.2407	3.3470
1	16.4114	13.3409	11.1801	3.2011	3.2654	3.3850

*Denotes literature value[64]

Table 3: Intermolecular free length and relaxation time of ZnO nanofluids at 298.15, 303.15 and 308.15 K

	$L_f \times 10^{11}$ (m)			$\tau \times 10^{12}$ (sec)		
Concentration (wt%)	298.15 K	303.15 K	308.15 K	298.15 K	303.15 K	308.15 K
0	3.7310	3.8014	3.8843	7.5682	6.1986	5.3387
0.2	3.7125	3.7844	3.8683	7.0098	5.7539	4.9931
0.4	3.6861	3.7588	3.8443	6.7749	5.5799	4.8687
0.6	3.6447	3.7221	3.8142	6.4435	5.3646	4.6961
0.8	3.6722	3.7365	3.8315	6.7069	5.5750	4.8606
1	3.6799	3.7507	3.8532	7.0045	5.8085	5.0460

hence, speed of sound increases upto 0.6 wt%. Further, as the concentration of nanoparticle increased, there is increase in the random motion of nanoparticles. When the ultrasonic wave propagates in nanofluid, Brownian motion stops the fluid molecules in nanofluid matrix and hence, speed of sound decreases beyond 0.6 wt% of ZnO nanoparticle loading. This indicates that decrease in the nanoparticle-fluid interaction and particle-particle interaction prevalence leads to decrease in speed of sound value. Further, increase in temperature causes more rapid movements of suspended particles in the dispersion, which results in increase in adiabatic compressibility (Table 2) and hence decreases in speed of sound (Table 1). So, this reveals that there is decrease in particle-fluid interaction at high temperatures. Also, a uniform decrease in density values with increase in temperature are observed (Table 1), which is again indicating the weakening of particle-fluid interactions due to thermal disturbance of the molecules at high temperatures.

An initial decrease in viscosity is observed upto critical concentration, 0.6 wt% (Table 2). As ZnO nanoparticles are added to ethylene glycol fluid, interaction between nanoparticles and ethylene glycol molecules on nanoparticle's surfaces may disturb the hydrogen bonding network of ethylene glycol molecules. These small perturbations in hydrogen bonding between ethylene glycol molecules[47,48] may result in viscosity reduction[49]. As more nanoparticles are loaded, more nanoparticle-ethylene glycol molecules interaction leads to enhancement of perturbations to the hydrogen bonding network of ethylene glycol and hence, viscosity decreases in the range of 0-0.6 wt%. However, beyond 0.6 wt% nanoparticle concentration increase in viscosity may be due to increased viscous dissipation due to addition of ZnO nanoparticles. Further, a decrease in viscosity is observed with increase in temperature, which indicates weakening of intermolecular forces (Table 2). Increased thermal energy of the system at high temperature may results in thermal agitation of the molecules and hence, decreases in viscosity values. A decrease in viscosity of liquids at high temperatures are observed due to decrease in the extent of intermolecular attractive forces such as hydrogen bonds[50]. Reduction in intermolecular forces of attraction at higher temperatures causes an increase in volume and hence, decreases in density and viscosity[51].

Adiabatic compressibility is calculated by using the Newton-laplace's Eq. 4[52,53]:

$$\beta_{ad} = \frac{1}{U^2\rho} \ (N^{-1} \ m^2) \tag{4}$$

where, U is speed of sound and ρ is density of nanofluid.

Intermolecular free length is determined using the following Eq. 5 given by Jacobson[54]:

$$L_f = K_T \beta_{ad}^{1/2} \ (m) \tag{5}$$

where, K_T is Jacobson's constant. This constant is a temperature dependent parameter, whose value at 298.15, 303.15 and 308.15 K is 2.0568×10^{-6}, 2.0756×10^{-6} and 2.0943×10^{-6}, respectively.

Adiabatic compressibility and intermolecular free length initially decreases upto 0.6 wt% and afterwards increases with increase in further nanoparticle loading (Table 2 and 3,

Table 4: Absorption coefficient and acoustic impedance of ZnO nanofluids at 298.15, 303.15 and 308.15 K

	$\alpha/f^2\times10^{14}$ (sec^2 m^{-1})			$Z\times10^{-6}$ (N sec m^{-3})		
Concentration (wt%)	298.15 K	303.15 K	308.15 K	298.15 K	303.15 K	308.15 K
0	9.0185	7.4459	6.4840	1.8365	1.8161	1.7905
0.2	8.3049	6.8765	6.0331	1.8442	1.8231	1.7960
0.4	7.9749	6.6300	5.8526	1.8586	1.8373	1.8092
0.6	7.5095	6.3194	5.6083	1.8822	1.8576	1.8259
0.8	7.8836	6.6003	5.8387	1.8700	1.8527	1.8200
1	8.2629	6.9115	6.1015	1.8689	1.8479	1.8115

Table 5: Gibb's free energy and free volume of ZnO nanofluids at 298.15, 303.15 and 308.15 K

	$G\times10^{21}$ (J mol^{-1})			$V_f\times10^{9}$ (m^3 mol^{-1})		
Concentration (wt%)	298.15 K	303.15 K	308.15 K	298.15 K	303.15 K	308.15 K
0	15.8437	15.3437	15.0312	1.6409	2.2512	2.8770
0.2	15.5283	15.0322	14.7465	1.8307	2.5045	3.1685
0.4	15.3881	14.9037	14.6392	1.9055	2.5937	3.2569
0.6	15.1817	14.7391	14.4857	2.0175	2.7085	3.3936
0.8	15.3465	14.9000	14.6322	1.9198	2.5689	3.2408
1	15.5252	15.0717	14.7914	1.8018	2.4267	3.0879

respectively). Decrease in adiabatic compressibility and intermolecular free length upto critical concentration shows a significant particle-fluid interaction[55]. It has previously been reported that adiabatic compressibility and intermolecular free length shows an contradictory behavior in comparison to speed of sound[56,57]. Further it can be seen that both adiabatic compressibility as well as intermolecular free length increases with temperature (Table 2 and 3, respectively). As temperature rises, thermal energy of the system increases, which leads to more spacing between the molecules. This may results in expansion of volume and hence, a consequent increase in adiabatic compressibility and intermolecular free length[58,59]. Relaxation time can be calculated from the Eq. 6[60]:

$$\tau = \left(\frac{4}{3}\right)\beta\eta \text{ (sec)} \tag{6}$$

An initial decrease in relaxation time upto critical concentration is observed (Table 3). This may be due to structural relaxation process[61] and hence, may lead to the rearrangement of molecules due to co-operative process[62]. Further relaxation time decreases with increase in temperature (Table 3). With rise in temperature, thermal energy of the system increases causing an increase in excitation energy and hence, fall in values of relaxation time at higher temperature[63].

Absorption coefficient can be calculated using the Eq. 7:

$$\left(\frac{\alpha}{f^2}\right) = 4\pi^2\frac{\tau}{2U} \text{ (sec}^2\text{ m}^{-1}\text{)} \tag{7}$$

A decrease in absorption coefficient below critical concentration can be seen beyond, which absorption coefficient increases (Table 4). Such decreasing trends further support the probability of strong particle-fluid interaction upto critical concentration[25]. However, beyond 0.6 wt%, increase in absorption coefficient indicates weak interactions between particles and base fluid molecules. Further increase in temperature results in decrease in absorption coefficient values (Table 4). Similar trends of absorption coefficient were reported earlier[63,65].

Acoustic impedance is calculted from Eq. 8[66]:

$$Z = Ux\rho \text{ (N sec m}^{-3}\text{)} \tag{8}$$

It is observed that acoustic impedance increases with increase in concentration of particles upto critical concentration and then it decreases with further nanoparticle loading (Table 4). So, variation of acoustic impedance goes parallel as that of speed of sound[56]. Such type of variations of acoustic impedance with concentration indicates significant interaction between the particle and base fluid molecules upto 0.6 wt% beyond, which particle-particle interaction predominates causing decrease in acoustic impedance. Further increase in temperature leads to reduction in acoustic impedance values (Table 4), which may be due to weakening of particle-fluid interactions at high temperatures.

Gibb's free energy is calculated from relaxation time (τ) as follows Eq. 9:

$$\Delta G = \kappa T \ln\left(\frac{\kappa T\tau}{h}\right) \text{(J mol}^{-1}\text{)} \tag{9}$$

Gibb's free energy initially decreases upto critical concentration and afterwards increases with increase in concentration (Table 5). So, Gibb's free energy shows

comparable behavior to that of relaxation time. Further Gibb's free energy decreases as temperature increases (Table 5). Increase in temperature causes an increase in kinetic energy of the molecules, which may delays the process of reorganization of molecules and hence, results in reduction in Gibb's free energy.

Free volume is calculated by following Eq. 10 obtained on the basis of dimension analysis[67]:

$$v_i = \left(\frac{M_{eff}U}{K\eta}\right) (m^3\ mol^{-1}) \quad (10)$$

where, M_{eff} is the effective molecular weight, which is expressed as $M_{eff} = \Sigma M = m_i x_i$, where, x and m are the mole fraction and molecular weight of the individual component in the mixture, respectively. The K is the temperature independent constant and its value is 4.28×10^9.

It can be seen that free volume first increase and after 0.6 wt% it decreases (Table 5). Increase in free volume with concentration indicates the interactions through hydrogen bonding[65] and shows the increasing extent of ZnO-ethylene glycol molecules interaction. However, decrease of particle-fluid interaction after 0.6 wt%, causes free volume to decrease. Further as the temperature is increased, increase in free volume is observed (Table 5). This may be due to increased chaos in the system because of increase in mobility of the molecules[68]. Similar trends were reported earlier[69].

CONCLUSION

Speed of sound, density and viscosity has been measured for different concentrations in ZnO-ethylene glycol nanofluid at temperatures 298.15, 303.15 and 308.15 K. Using the experimental data, various acoustical parameters were evaluated and particle-particle and particle-fluid interactions were analyzed. Speed of sound increases with increase in concentration up to a critical concentration of 0.6 wt% due to increase in particle-fluid interaction but beyond this critical concentration, there is strong particle-particle interaction and weaker particle-fluid interaction. Further, particle-fluid interaction decreases at higher temperatures leading to decrease in values of speed of sound. So, the analysis of variation of all the evaluated acoustical parameters shows that interaction between ZnO nanoparticles becomes predominant after 0.6 wt% due to agglomeration. Significant interaction between ZnO nanoparticles and ethylene glycol molecules favors an increase in speed of sound. Such particle-fluid interaction studies are supportive to answer the significant enhancements in physical properties of nanofluids and also to realize the mechanism of fluid flow in nanoscale. So it may be concluded that the concentration of ZnO-ethylene glycol nanofluid upto 0.6 wt%, in which nanoparticle-fluid interaction is significant and highly suitable for their applicability.

ACKNOWLEDGMENTS

The authors are thankful to Department of Chemistry (University of Jammu) for providing necessary facilities and support for conducting present study and CSIR UGC for Junior Research Fellowship (JRF) to the first author. The authors gratefully acknowledge SAIF STIC (Kochi), SAIF Chandigarh, CIL Chandigarh for providing the facilities for characterization.

REFERENCES

1. Wan, M., R.R. Yadav, K.L. Yadav and S.B. Yadaw, 2012. Synthesis and experimental investigation on thermal conductivity of nanofluids containing functionalized Polyaniline nanofibers. Exp. Thermal Fluid Sci., 41: 158-164.
2. Choi, S.U.S., 1995. Enhancing Thermal Conductivity of Fluids with Nanoparticles. In: Developments and Applications of Non-Newtonian Flows, Siginer, D.A. and H.P. Wang (Eds.). Vol. 231, ASME, New York, pp: 99-105.
3. Li, Y., J. Zhou, S. Tung, E. Schneider and S. Xi, 2009. A review on development of nanofluid preparation and characterization. Powder Technol., 196: 89-101.
4. Eastman, J.A., S.U.S. Choi, S. Li, W. Yu and L.J. Thompson, 2001. Anomalously increased effective thermal conductivities of ethylene glycol-based nanofluids containing copper nanoparticles. Applied Phys. Lett., 78: 718-720.
5. Lo, C.H., T.T. Tsung, L.C. Chen, C.H. Su and H.M. Lin, 2005. Fabrication of copper oxide nanofluid using Submerged Arc Nanoparticle Synthesis System (SANSS). J. Nanoparticle Res., 7: 313-320.
6. Zhu, H.T., Y.S. Lin and Y.S. Yin, 2004. A novel one-step chemical method for preparation of copper nanofluids. J. Colloid Interface Sci., 277: 100-103.
7. Xuan, Y. and Q. Li, 2000. Heat transfer enhancement of nanofluids. Int. J. Heat Fluid Flow, 21: 58-64.
8. Ruan, B. and A.M. Jacobi, 2012. Ultrasonication effects on thermal and rheological properties of carbon nanotube suspensions. Nanoscale Res. Lett., Vol. 7. 10.1186/1556-276X-7-127
9. Choi, S.U.S., Z.G. Zhang, W. Yu, F.E. Lockwood and E.A. Grulke, 2001. Anomalous thermal conductivity enhancement in nanotube suspensions. Applied. Phys. Lett., 79: 2252-2254.
10. Das, S.K., N. Putra, P. Thiesen and W. Roetzel, 2003. Temperature dependence of thermal conductivity enhancement for nanofluids. J. Heat Transfer, 125: 567-574.

11. Kumar, D.H., H.E. Patel, V.R. Kumar, T. Sundararajan, T. Pradeep and S.K. Das, 2004. Model for heat conduction in nanofluids. Phys. Rev. Lett., Vol. 93. 10.1103/PhysRevLett.93.144301
12. Jang, S.P. and S.U.S. Choi, 2004. Role of Brownian motion in the enhanced thermal conductivity of nanofluids. Applied Phys. Lett., Vol. 84. 10.1063/1.1756684
13. Koo, J. and C. Kleinstreuer, 2004. A new thermal conductivity model for nanofluids. J. Nanoparticle Res., 6: 577-588.
14. Prasher, R., P. Bhattacharya and P.E. Phelan, 2005. Thermal conductivity of nanoscale colloidal solutions (nanofluids). Phys. Rev. Lett., Vol. 94. 10.1103/PhysRevLett.94.025901
15. Prasher, R., P. Bhattacharya and P.E. Phelan, 2005. Brownian-motion-based convective-conductive model for the effective thermal conductivity of nanofluids. J. Heat Transfer, 128: 588-595.
16. Chon, C.H. and K.D. Kihm, 2005. Thermal conductivity enhancement of nanofluids by Brownian motion. J. Heat Transfer, Vol. 127. 10.1115/1.2033316
17. Xuan, Y., Q. Li, X. Zhang and M. Fujii, 2006. Stochastic thermal transport of nanoparticle suspensions. J. Applied Phys., Vol. 100. 10.1063/1.2245203
18. Singh, A.K., 2008. Thermal conductivity of nanofluids. Defence Sci. J., 58: 600-607.
19. Sayan, P. and J. Ulrich, 2002. The effect of particle size and suspension density on the measurement of ultrasonic velocity in aqueous solutions. Chem. Eng. Process.: Process Intensif., 41: 281-287.
20. Yadav, R.R., G. Mishra, P.K. Yadava, S.K. Kor, A.K. Gupta, B. Raj and T. Jayakumar, 2008. Ultrasonic properties of nanoparticles-liquid suspensions. Ultrasonics, 48: 591-593.
21. Hornowski, T., A. Jozefczak, M. Labowski and A. Skumiel, 2008. Ultrasonic determination of the particle size distribution in water-based magnetic liquid. Ultrasonics, 48: 594-597.
22. Motozawa, M., Y. Iizuka and T. Sawada, 2008. Experimental measurements of ultrasonic propagation velocity and attenuation in a magnetic fluid. J. Phys. Condens. Matter, Vol. 20. 10.1088/0953-8984/20/20/204117
23. Singh, D.K., D.K. Pandey and R.R. Yadav, 2009. An ultrasonic characterization of ferrofluid. Ultrasonics, 49: 634-637.
24. Rashin, M.N., J. Hemalatha, R.P. Nalini and A.V. Ramya, 2011. Ultrasonic studies and microchannel flow behavior of copper oxide nanofluid. AIP Conf. Proc., 1349: 335-336.
25. Hemalatha, J., T. Prabhakaran and R.P. Nalini, 2011. A comparative study on particle-fluid interactions in micro and nanofluids of aluminium oxide. Microfluidics Nanofluidics, 10: 263-270.
26. Rashin, M.N. and J. Hemalatha, 2012. Acoustic study on the interactions of coconut oil based copper oxide nanofluid. Int. J. Eng. Applied Sci., 6: 216-220.
27. Rashin, M.N. and J. Hemalatha, 2013. Acoustical Studies of the Intermolecular Interaction in Copper Oxide-Ethylene Glycol Nanofluid. In: Advanced Nanomaterials and Nanotechnology, Giri, P.K., D.K. Goswami and A. Perumal (Eds.). Springer, New York, USA., ISBN-13: 9783642342165, pp: 225-229.
28. Kiruba, R. and A.K.S. Jeevaraj, 2014. Effect of temperature and concentration on the molecular interactions of Cu/ZnO-EG nanofluids using ultrasonic study. Integr. Ferroelectr., 150: 59-65.
29. Rashin, M.N. and J. Hemalatha, 2014. Magnetic and ultrasonic studies on stable cobalt ferrite magnetic nanofluid. Ultrasonics, 54: 834-840.
30. Patel, J.K. and K. Parekh, 2015. Effect of carrier and particle concentration on ultrasound properties of magnetic nanofluids. Ultrasonics, 55: 26-32.
31. Zafarani-Moattar, M.T. and R. Majdan-Cegincara, 2012. Effect of temperature on volumetric and transport properties of nanofluids containing ZnO nanoparticles poly (ethylene glycol) and water. J. Chem. Thermodyn., 54: 55-67.
32. Seow, Z.L.S., A.S.W. Wong, V. Thavasi, R. Jose, S. Ramakrishna and G.W. Ho, 2008. Controlled synthesis and application of ZnO nanoparticles, nanorods and nanospheres in dye-sensitized solar cells. Nanotechnology, Vol. 20. 10.1088/0957-4484/20/4/045604/meta
33. Rasmussen, J.W., E. Martinez, P. Louka and D.G. Wingett, 2010. Zinc oxide nanoparticles for selective destruction of tumor cells and potential for drug delivery applications. Expert Opin. Drug Delivery, 7: 1063-1077.
34. Meruvu, S., L. Hugendubler and E. Mueller, 2011. Regulation of adipocyte differentiation by the zinc finger protein ZNF638. J. Biol. Chem., 286: 26516-26523.
35. Mansour, A.F., S.F. Mansour and M.A. Abdo, 2015. Improvement structural and optical properties of ZnO/PVA nanocomposites. J. Applied Phys., 7: 60-69.
36. Patterson, A.L., 1939. The Scherrer formula for X-ray particle size determination. Phys. Rev., 56: 978-982.
37. Rezende, C.P., J.B. da Silva and N.D.S. Mohallem, 2009. Influence of drying on the characteristics of zinc oxide nanoparticles. Braz. J. Phys., 39: 248-251.
38. Zak, A.K., M.E. Abrishami, W.H.A. Majid, R. Yousefi and S.M. Hosseini, 2011. Effects of annealing temperature on some structural and optical properties of ZnO nanoparticles prepared by a modified sol-gel combustion method. Ceram Int., 37: 393-398.
39. Soosen, S.M., B. Lekshmi and K.C. George, 2009. Optical properties of Zno nanoparticles. Acad. Rev., 16: 57-65.
40. Bagheri, S., K.G. Chandrappa and S.B.A. Hamid, 2013. Facile synthesis of nano-sized ZnO by direct precipitation method. Der Pharma Chemica, 5: 265-270.
41. Yadav, R.S., P. Mishra and A.C. Pandey, 2008. Growth mechanism and optical property of ZnO nanoparticles synthesized by sonochemical method. Ultrason. Sonochem. 15:: 863-868.
42. Tauc, J., 1968. Optical properties and electronic structure of amorphous Ge and Si. Mat. Res. Bull., 3: 37-46.
43. Berger, L.I., 1997. Semiconductor Materials. CRC Press, Boca Raton, FL., USA., ISBN-13: 9780849389122, Pages: 496.

44. Yang, J., F.C. Meldrum and J.H. Fendler, 1995. Epitaxial growth of size-quantized cadmium sulfide crystals under arachidic acid monolayers. J. Phys. Chem., 99: 5500-5504.
45. Thirumaran, S. and S. Sudha, 2010. Intermolecular interaction studies in organic ternary liquid mixtures by ultrasonic velocity measurements. J. Chem. Pharmaceut. Res., 2: 327-337.
46. Kiruba, R., M. Gopalakrishnan, T. Mahalingam, A. Jeevaraj and A.K. Solomon, 2012. Ultrasonic studies on zinc oxide nanofluids. J. Nanofluids, 1: 97-100.
47. Tan, Y., Y. Song and Q. Zheng, 2012. Hydrogen bonding-driven rheological modulation of chemically reduced graphene oxide/poly (vinyl alcohol) suspensions and its application in electrospinning. Nanoscale, 4: 6997-7005.
48. Chaplin, M., 2007. Water's hydrogen bond strength. Condensed Matter. http://arxiv.org/ftp/arxiv/studys/0706/0706.1355.pdf.
49. Suganthi, K.S., V.L. Vinodhan and K.S. Rajan, 2014. Heat transfer performance and transport properties of ZnO-ethylene glycol and ZnO-ethylene glycol-water nanofluid coolants. Applied Energy, 135: 548-559.
50. Rashin, M.N. and J. Hemalatha, 2013. Viscosity studies on novel copper oxide-coconut oil nanofluid. Exp. Thermal Fluid Sci., 48: 67-72.
51. Praharaj, M.K., A. Satapathy, P. Mishra and S. Mishra, 2013. Ultrasonic analysis of intermolecular interaction in the mixtures of benzene with N, N-dimethylformamide and cyclohexane at different temperatures. J. Chem. Pharmaceut. Res., 5: 49-56.
52. Rowlinson, J.S., F.L. Swinton, J.E. Baldwin, A.D. Buckingham and S. Danishefsky, 1982. Liquids and Liquid Mixtures. 3rd Edn., Butterworths, London, UK., ISBN: 978-0-408-24193-9 pp: 16.
53. Povey, M.J.W., 1997. Ultrasonic Techniques for Fluids Characterization. 1st Edn., Academic Press, USA., ISBN-13: 978-0125637305 pp: 25.
54. Jacobson, B., 1951. Intermolecular free lengths in liquids in relation to compressibility, surface tension and viscosity. Acta Chemica Scandinavica, 5: 1214-1216.
55. Gupta, V., U. Magotra, Sandarve, A.K. Sharma and M. Sharma, 2015. CuO nanofluids: Particle-fluid interaction study using ultrasonic technique. J. Chem. Pharmaceut. Res., 7: 313-326.
56. Gupta, V., A.K. Sharma and M. Sharma, 2014. Ultrasonic investigation of molecular interaction in aqueous glycerol and aqueous ethylene glycol solution. J. Chem. Pharmaceut. Res., 6: 714-720.
57. Gupta, V., A.K. Sharma and M. Sharma, 2014. Comparative ultrasonic and conductometric studies of aqueous sodium chloride and potassium chloride solutions. Chem. Sci. Trans., 3: 736-744.
58. Praharaj, M.K., P. Mishra, S. Mishra and A. Satapathy, 2012. Study of thermodynamic and transport properties of ternary liquid mixture at different temperatures. Adv. Applied Sci. Res., 3: 1518-1530.
59. Panda, S. and A.P. Mahapatra, 2014. Variation of thermo-acoustic parameters of dextran with concentration and temperature. J. Chem. Pharmaceut. Res., 6: 818-825.
60. Hildebrand, J.H., 1959. Free volumes in liquids. J. Chem. Phys., 31: 1423-1425.
61. Kinsler, L.E. and A.R. Fray, 1989. Fundamentals of Acoustics. Wiley Eastern, New Delhi, India.
62. Ali, A., S. Hyder and A.K. Nain, 2000. General physics-intermolecular interactions in ternary liquid mixtures by ultrasonic velocity measurements. Indian J. Phys., 74: 63-68.
63. Umadevi, M. and R. Kesavasamy, 2012. Thermodynamics and transport properties of ester with cyclohexane in pentanol at 303, 308 and 313 K. Int. J. Res. Chem. Environ., 2: 157-163.
64. Pastoriza-Gallego, M.J., L. Lugo, J.L. Legido and M.M. Pineiro, 2011. Thermal conductivity and viscosity measurements of ethylene glycol-based Al_2O_3 nanofluids. Nanoscale Rese. Lett., Vol. 6. 10.1186/1556-276X-6-221
65. Naik, R.R., S.V. Bawankar and V.M. Ghodki, 2015. Acoustical studies of molecular interactions in the solution of anti-malarial drug. J. Polym. Biopolym. Phys. Chem., 3: 1-5.
66. Prigogine, L. and V. Malhot, 1957. The Molecular Theory of the Solution. North-Holland Publishing Company, New York, Pages: 448.
67. Suryanarayana, C.V. and J. Kuppusamy, 1976. Free volume and internal pressure of liquid from ultrasonic velocity. J. Acoust. Soc. Ind., 4: 75-75.
68. Chimankar, O.P., R. Shriwas and V.A. Tabhane, 2011. Intermolecular interaction studies in some amino acids with aqueous NaOH. J. Chem. Pharm. Res., 3: 587-596.
69. Umadevi, M. and R. Kesavasamy, 2012. Molecular interaction studies on ester with cyclohexane in alcohol at 303, 308 and 313 K. Int. J. Chem. Environ. Pharmaceut. Res., 3: 72-78.